

Application of some carbon-aluminium based nanostructures obtained by TVA method in divertors coating from fusion reactor

Ș.G.TUTUN^{a*}, L. PETRĂȘESCU^a, R. VLĂDOIU^b, G. PRODAN^b, C. P. POROȘNICU^c, E. VASILE^d, I. PRIOTEASA^a, R. MANU^a, V. CIUPINĂ^{b,e}.

^aFaculty of Physics, University of Bucharest, Atomistilor 405, Măgurele, Ilfov

^bOvidius University of Constanta, Mamaia 124, Constanța, 900527, Romania

^cNational Institute for Laser, Plasma and Radiation Physics, PO Box MG-36, 077125, Bucharest, Romania

^dUniversity Politehnica of Bucharest, No. 1-7 Gh. Polizu Street, Bucharest 011061, Romania

^eAcademy of Romanian Scientists, Independenței 54, Bucharest 050094, Romania

Nanostructured carbon materials have increasingly attracted the interest of the scientific community, because of their physical properties and potential application in high-tech devices. In the current ITER design, the tiles made of carbon fiber composites (CFCs) are foreseen for the strike point zone and tungsten (W) for other parts of the divertor region. This choice is a compromise based mainly on experience with individual materials in many different tokamaks. Also C-Al composites are the candidate material for this first Wall in ITER. In order to prepare nanostructured carbon based nanocomposite for the divertor part in fusion application, the Thermionic Vacuum Arc (TVA) method was used in two electronic gun configuration. One of the main advantages of this technology is the bombardment of the growing thin film just by the ions of the depositing material. Even more, the energy of ions can be controlled. Thermo-electrons emitted by an externally heated cathode and focused by a Wehnelt focusing cylinder are strongly accelerated towards the anode whose material is evaporated and bright plasma is ignited by a high voltage DC supply. The nanostructured amorphous C-Al samples were characterized by Transmission Electron Microscopy (TEM), Scanning Electron Microscopy (SEM), Energy Dispersive X-ray Spectroscopy (EDXS) and magnetoresistance analysis. The carbon based nanostructures were identified by TEM and SEM as having a uniform morphology and amorphous structure. The EDXS method confirms the presence of the C, Al and Si in the samples. The electric measurements shows the resistance differences in the analyzed samples and that, in conclusion, the Al concentration and the type of the surface have a matter in the electric resistance effect. Also, in the presence of a magnetic field of 0.3T all the thin films that were investigated showed a slight drop in resistance.

(Received December 10, 2014; accepted June 24, 2015)

Keywords: divertor, C-Al, TVA, TEM, Electron diffraction, SEM, EDXS, Magnetoresistance, coating

1. Introduction

The experimental development of control fusion nuclear reactor it's an extreme difficult task. For the ITER design, combinatorial deposition of thin films made of two components are used to obtain structures that exhibit similar features to those deposited in different parts of the fusion reactor [1], [2].

If used at the divertor, this type of thin films, can generate thermonuclear reactor operating conditions where part of the wall is covered with tiles made out of carbon and beryllium [3]. Their interaction with the high-energy plasma leads to migration and the mixture of these elements in unwanted places. Also, Be layers will not be suitable due to radiation damage and similarly, a single carbon surface will not be suitable due to high physical and chemical sputtering rates [4].

A possible solution for coating the divertor is to use the combination of C-Al thin films. For this we need a solution for material synthesis and also to find the correct concentration between carbon and aluminum [5-7].

Our goal is to exchange, if possible, C-Be thin films with equivalent C-Al thin films. The aluminum is not flammable, but the aluminum powder is. The range of ignition temperature is depending of morphological features, ranging between 300 - 600 °C for the layer, and 650 - 700 °C for cloud aluminum powder. Another infringement is toxicity, beryllium being rated as a potential carcinogen and it must be label properly. Aluminum materials are not label so [6].

So, we need to create C-Al nanocomposites coatings design to have excellent tribological properties while the structure in composed by nanocrystals complex surrounded by amorphous structures with a strong graphitization tendency, allowing the creation of adherent and wear resistant films [6].

This C-Al material should be capable of withstanding high performance plasma discharges and disruptions, while retaining the capability of transmitting high-grade heat for power conversion [8], [9].

We can also see that the TVA method is suitable for the synthesis of C-Al deposition films [6], and more

important, is a low cost method that allows variation of concentration in one shot deposition [6,10, 11, 12].

2. Materials and methods

The carbon nanocomposites thin films have been obtained by TVA method using a double source configuration, one for atomize carbon rods, and second for aluminum powder. The setup was used for the deposition of the C - Al thin films on silicon substrate.

The internal pressure was around the value of $5 \cdot 10^{-6}$ Torr. Filament current intensity had a value of 43A for the whole 28 min deposition time. A film of 4000 Å was obtained and the deposition ratio of C:Al was 1:7.5. Different C-Al thin films of various concentrations were obtained. The TVA sensor deposition and the math due to the geometrical position showed the difference in concentration between the two analyzed samples: *Sample S1*-(6,12%C; 93,88%Al); *Sample S2*-(16%C; 84%Al).

The two thin film samples (sample S1 and sample S2) were investigated using TEM, SEM, EDXS and magneto-resistance analysis to obtain information about morphology, crystalline structure, elemental composition and electrical properties.

The TEM studies were performed on Philips CM120ST with Megaview III CSD camera (at different magnification) with sample prepared by scratch method. For morphological characterization we assume a lognormal distribution of measured sizes of identified nanoparticles and Feret diameter to estimate those sizes. The experimental histogram was fit with user built lognormal function in SCIDavis application.

Ohmic contacts were attached on the samples for use in the electrical measurements. The electrical contact on the samples was performed by a product consisting of 80% silver-filled two-component epoxy-based glue (0.0025 Ω/cm specific resistance) [13].

And now this distance, between contacts, it's going to be considered the main electrical resistance.

3. Results and discussion

The morphology of samples was studied using TEM images. **Fig.1a**, **Fig.1a'** and **Fig.1b** illustrates the two nanostructures C-Al samples grown on a Si substrate, the samples thickness being of 400nm. The TEM voltage acceleration is 100kV and we have obtained morphological images and electron diffraction images of Samples S1 and S2.

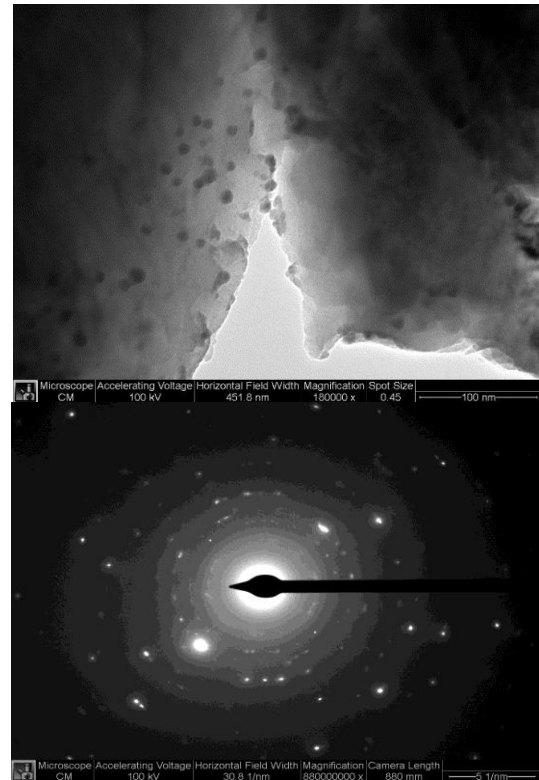


Fig.1a TEM and electron diffraction analysis (Sample S2)

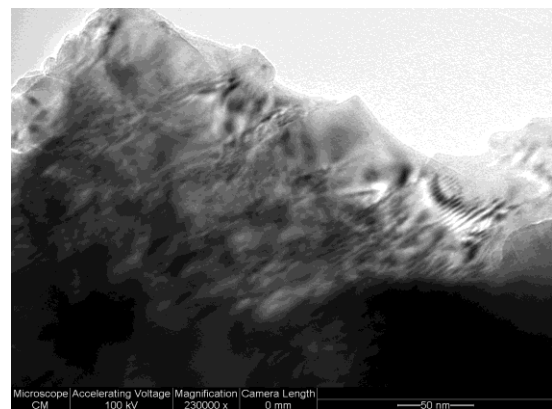


Fig.1a' TEM and electron diffraction analysis (Sample S2)

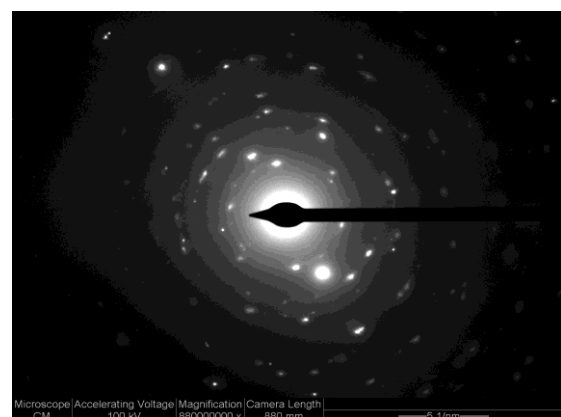


Fig.1b TEM and electron diffraction analysis (Sample S1)

The carbosn based nanostructures were identified by TEM as having an uniform morphology and amorphous structure and reveals that Al also crystallizes in small isles.

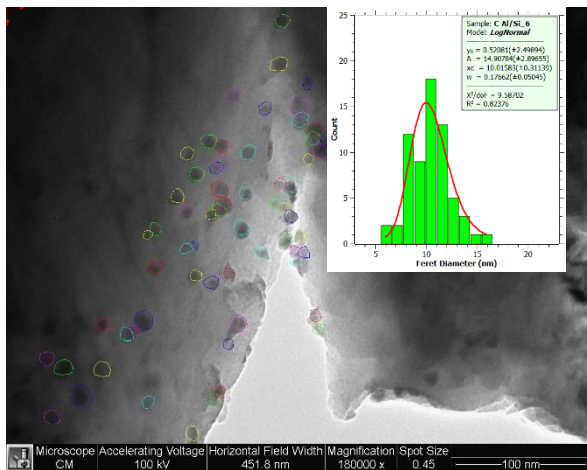


Fig.2 TEM analysis (Sample S2)

In Fig.2 we can observe that the Al crystallizes in small isles with a mean size/diameter of 10nm, measured using a density distribution.

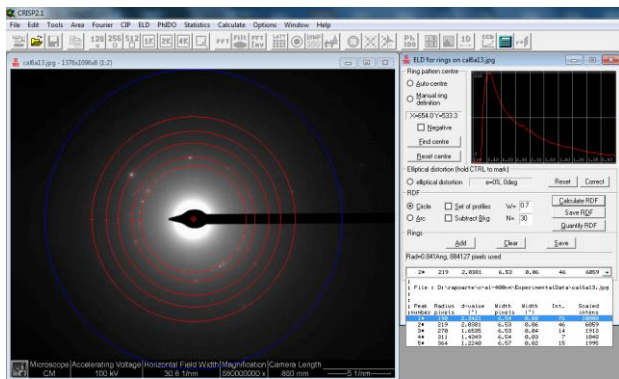


Fig.3 Electron diffraction pattern for C-Al/Si (Sample S2)

Using the classical electron diffraction analysis for sample S2 (Fig.3), we can determine for aluminum a lattice parameter of 1.75Å. The identified rings are shown in Tab.1. Electron diffraction shows the presence of a polycrystalline material, the predominant being the cubic phase.

For sample S1 the patterns contains mainly amorphous structures or as we can see in Fig.1b very small nanoparticles, so contribution to electron diffraction cannot be identified as diffraction rings.

Table 1. Peak selected for Al/Si indexing procedure (sample S2)

Peak	d(Å)	2θ(°)	10000*I/Imax	hkl	Phase
1	2.3421	0.753502	10000	111	Al
2	2.0381	0.87111	6059	200	Al
3	1.6535	1.238416	1913	113	Si
4	1.4349	1.449337	1048	220	Al
5	1.224	1.521773	1995	113	Al

The Scanning Electron Microscopy studies were performed on a SEM QUANTA INSPECT F, with the samples prepared by scratch method at on acceleration voltage of 30KV, at different magnification.

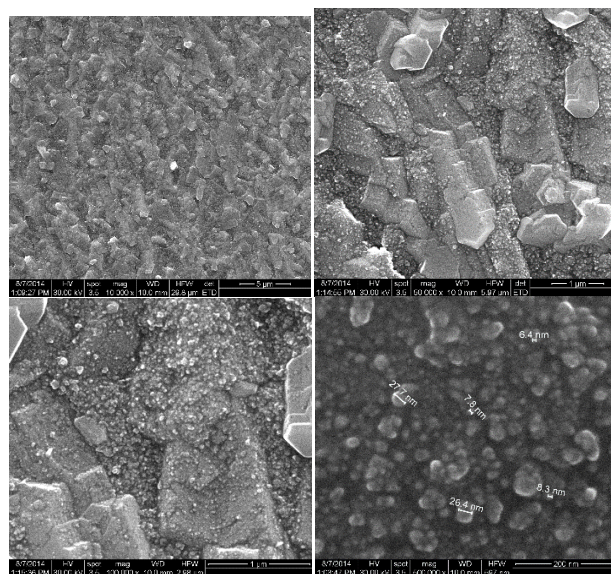


Fig.4a SEM analysis with different magnification on Sample S2 (10.000x - top left, 50.000x - top right, 100.000x - bottom left, 500.000x - bottom right)

On the first image from Fig.4a (10.000x - top left) we can see an uniform general aspect with an amorphous structure. When we move on to the second image (50.000x - top right) we can observe an irregular surface with Al isles (grains), most likely with a crystalline structure, suggested by the polyhedral shape of the Al grains with an average size of 300 nm. This is also confirmed by the next image (100.000x - bottom left). On both image we can observe the presence of two main phases: the crystallin polyhedral phase and the nano structure phase. These two phases can be mixt in between all the film layers depositions. The last image (500.000x - bottom right) indicates the average size of the nano structure phase in between 6 and 40 nm and has an irregular aspect with a grain structure.

This next set of images (Fig.4b) refers to sample S1 and represents the analogous comparison of sample S2. The first image (10.000x - top left) shows a general aspect on the C-Al film and as sample S2 it has an uniform general amorphous structure. We can see from the second and the third images (50.000x - top right and 100.000x - bottom left) reveals the same type of structure with the two main phases: the crystalline polyhedral phase and the nano grains structure phase. But, as a main difference, in this sample the crystalline polyhedral phase has a lower proportion compare to the polyhedric phase of sample S2. Also, as in sample S2, the Al grains have an average size of 300 nm. The fourth image (500.000x - bottom right) indicates the size of the nano particles in between 6 and 16 nm and that the nano structure particles covers most of the crystalline Al polyhedric phase.

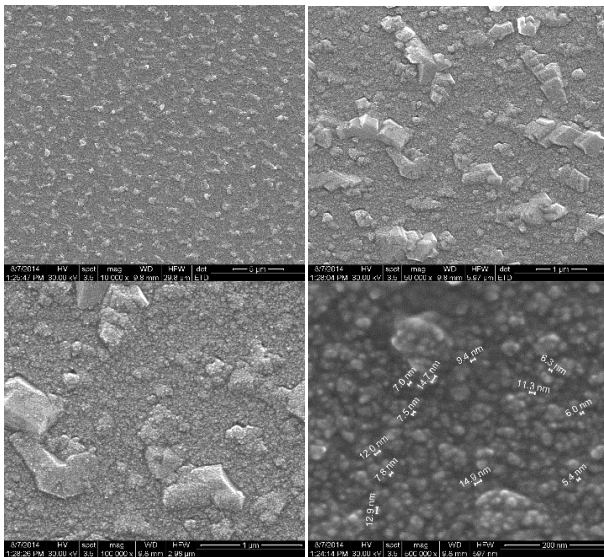


Fig.4b SEM analysis with different magnification on Sample S1 (10.000x - top left, 50.000x - top right, 100.000x - bottom left, 500.000x - bottom right)

The SEM it's also fitted with an X ray spectrometer with energy dispersion, EDXS. On both samples we have done X ray qualitative micro analysis, in order to identify the chemical elements presents in the examined samples.

The EDXS analysis for both Samples S1 and Sample S2 (in Fig.5a - sample S2, 5b - sample S1) reveals and confirms the presence of Al, C and Si (the support grid). The Al peak is found below the value of 1.6 keV, the Si peak right above the same value and the C one is situated right near the 0 value. Also, we note the presence of oxygen, that can be found on the surface of the film.

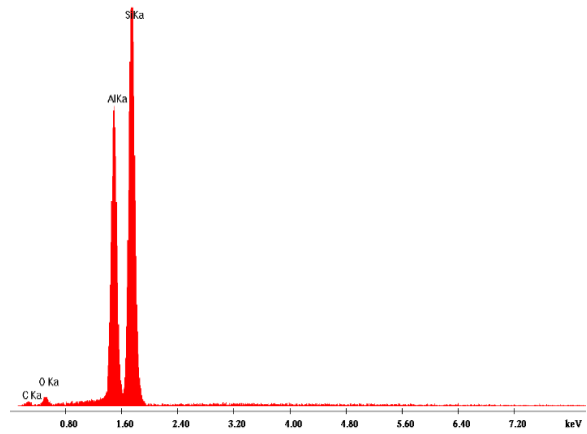


Fig.5a EDXS analysis for Sample S2

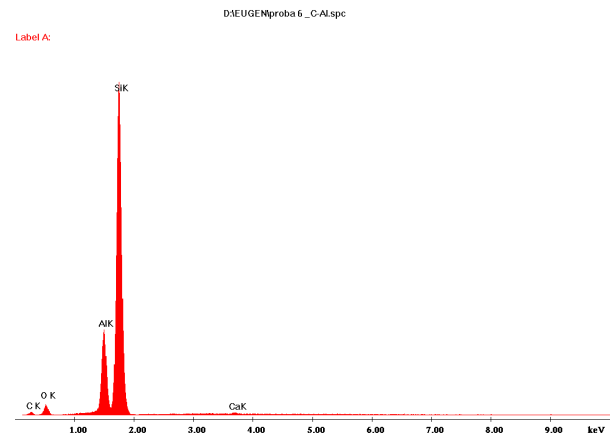


Fig.5b EDXS analysis for Sample S1

By correlating altogether the EDXS and TEM analysis we can see that crystallite isles of Al in sample S2 are slightly bigger than the ones in sample S1 and the Al isles in sample S1 tend to be more similar by size and shape.

Electrical conductivity was measured comparing the potential drop on the sample with the potential drop on a series resistance in constant current mode [13].

Fig.6 shows how the resistance of Sample S2, which has a thickness of about 400nm, is affected by temperature (without a magnetic field). It can be seen that the increase in temperature reveals an increase in resistance.

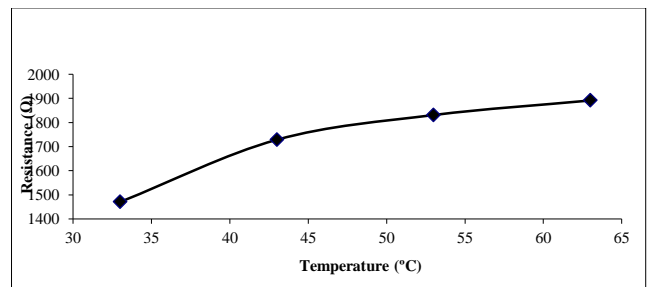


Fig.6 Resistance vs. temperature for Sample S2

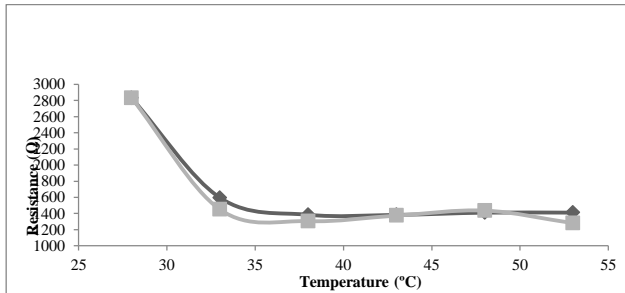


Fig.7 Resistance vs. temperature for Sample S1; (◇) without magnetic field, (□) in magnetic field ($B=0.33T$)

Fig.7 shows the Resistance vs. Temperature graph for Samples S1 with and without a magnetic field.

In the presence of a magnetic field of 0.33T the investigated sample has a small variation versus the temperature axis with a slightly drop of resistance. This implies that the magneto-resistive effect it's minimal.

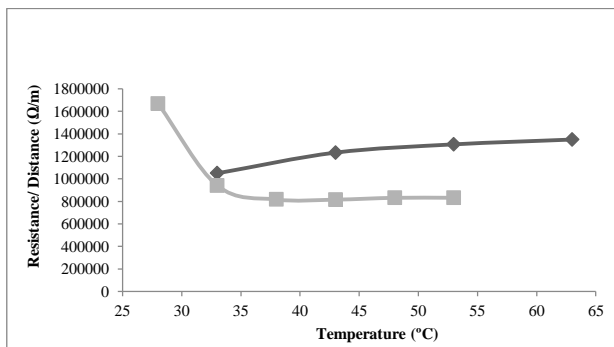


Fig.8 Resistance / distance between contacts ratio vs. temperature; (□)sample S1, (◇)sample S2.

In Fig.8 we observe a resistance comparison between sample S2 and sample S1 versus temperature. For the correct comparison it has been created a resistance per distance ratio for the two analyzed thin films. Sample S2 has higher resistance per distance ratio compare to Sample S1. If we check the TVA deposition parameters, this is consistent with the results, because the Al concentration of Sample S1 is higher than Al concentration of Sample S2.

4. Conclusions

Both examined samples have an uniform general morphology aspect with an amorphous structure confirmed by TEM and SEM analysis. Also, on both thin films we can observe the presence of two main phases: the crystallin polyhedric phase and the nano grains structure phase. But, as a main difference, in sample S2 the crystalline polyhedric phase has a higher proportion compare to the polyhedric phase of sample S1, where the nano grains phase it's predominant.

According to the electric mesuraments, sample S1 has a lower resistance per distance ratio in between contacts compare to sample S2. This is in agreement with the

samples concentrations, because the Al concentration of Sample S1 is higher than Sample S2.

Also, the samples sufaces have a matter in the electric resistance effect. Sample S1 has smaller average nanoparticles and less Al crystalites isles/grains, so it has a higher electric contact surface. This implies that the shape of the samples it is also an electric factor. We can conclude from here that the electric resistance is a factor determined by Al samples concentration and also it depends of the way the Al was deposit on the surface.

References

- [1] V. Ciupina, I.G. Morjan, R. Alexandrescu, F.V. Dumitrache, G Prodan., C. Lungu, R. Vladoiu, I. Mustata, V. Zarovschi, J. Sullivan, S. Saied, E. Vasile, I. Oancea-Stanescu, M. Prodan, D. Manole, A. Mandes, V. Dinca, M. Contulov, Proceedings of SPIE-The International Society for Optical Engineering, 7764, 77640O, Conference on Nanoengineering - Fabrication, Properties, Optics, and Devices VII, ed. by E.A. Dobisz, L.A. Eldada (2010).
- [2] S. Lehto, J. Likonen, J.P. Coad, T. Ahlgren, D.E. Hole, M. Mayer, H. Maier, J. Kolehmainen; Fusion Eng. Des. **66-68**, 241 (2003);
- [3] D. Lupton; 11 Beryllium in Landolt-Bornstein – Group VIII Advanced Materials and Technologies: Powder Metallurgy Data, 2A1, ed. by P. Beiss, R. Ruthardt, H. Warlimont, Springer-Verlag, Heidelberg, 2003;
- [4] C.P.C. Wong, J. Nucl. Mater. **390-391**, 1026 (2009).
- [5] V. Ciupina, I. Morjan, C.P. Lungu, R. Vladoiu, G. Prodan, M. Prodan, V. Zarovschi, C. Porosnicu, I.M. Stanescu, M. Contulov, A. Mandes, V. Dinca, K. Sugiyama, Proceedings of SPIE, 8104, 810411, Conference on Nanostructured Thin Films IV, ed. by, R.J. MartinPalma Y.J. Jen, T.G. Mackay (2011);
- [6] V. Ciupina, C.P. Lungu, R. Vladoiu, T.D. Epure, G. Prodan, C. Porosnicu, M. Prodan, I.M. Stanescu, M. Contulov, A. Mandes, V. Dinca, V. Zarovschi, Proceedings of SPIE, 8465, 846508, Conference on Nanostructured Thin Films V, ed. by T.G. Mackay, Y.J. Jen, R.J. MartinPalma (2012);
- [7] G. Musa, I. Mustata, V. Ciupina, R. Vladoiu, G. Prodan, E. Vasile, H. Ehrich, Diam. Relat. Mater. **13**, 1398 (2004);
- [8] A. Litnovsky, D.L. Rudakov, G. De Temmerman, P. Wienhold, V. Philipps, U. Samm, A.G. McLean, W.P. West, C.P.C. Wong, N.H. Brooks, J.G. Watkins, W.R. Wampler, P.C. Stangeby, J.A. Boedo, R.A. Moyer, S.L. Allen, M.E. Fenstermacher, M. Groth, C.J. Lasnier, R.L. Boivin, A.W. Leonard, A. Romanyuk, T. Hirai, G. Pintsuk, U. Breuer, A. Scholl, Fusion Eng. Des. **83**, 79 (2008);
- [9] T.K. Gray, R. Maingib, J.E. Surany, J. Nucl. Mater. **363-365**, 196 (2007);

- [10] R. Vladoiu, V. Ciupina, C. Surdu-Bob, C.P. Lungu, J. Janik, J.D. Skalny, V. Bursikova, J. Bursik, G. Musa, *J. Optoelectron. Adv. Mater.* **9**, 862 (2007);
- [11] R. Vladoiu, V. Ciupina, A. Mandes, V. Dinca, M. Prodan, G. Musa, *J. Appl. Phys.* **108**, 093301 (2010);
- [12] V. Ciupina, R. Vladoiu, C.P. Lungu, V. Dinca, M. Contulov, A. Mandes, P. Popov, G. Prodan, *Eur. Phys. J. D* **66**, 99 (2012);
- [13] V. Ciupina, C.P. Lungu, R. Vladoiu, G.C. Prodan, S. Antohe, C. Porosnicu, I. Stanescu, I. Jecu, S. Iftimie, M. Prodan, A. Mandes, V. Dinca, E. Vasile, V. Zarovski, V. Nicolescu, *Proceedings of SPIE*, 9172, 91720Y, Conference on Nanostructured Thin Films VII, ed. by A. Lakhtakia, T.G. Mackay, M. Suzuki (2014).

*Corresponding author: gabi_cga_85@yahoo.com